Human Molecular Genetics, 2013, Vol. 22, No. 25 **5188–5198**
doi:10.1093/hmg/ddt373
Advance Access published on August 6, 2013

A defective Krab-domain zinc-finger transcription factor contributes to altered myogenesis in myotonic dystrophy type 1

Morgane Gauthier[1,2], Antoine Marteyn[1,2], Jérôme Alexandre Denis[1,2], Michel Cailleret[1,2], Karine Giraud-Triboult[3], Sophie Aubert[3], Camille Lecuyer[3], Joelle Marie[4], Denis Furling[5], Rémi Vernet[6], Clara Yanguas[1,2], Christine Baldeschi[1,2], Geneviève Pietu[1,2], Marc Peschanski[1,2] and Cécile Martinat[1,2,*]

[1]INSERM UMR 861, I-Stem AFM, Evry Cedex 91030, France, [2]UEVE UMR 861 I-Stem AFM, Evry Cedex 91030, France, [3]CECS/I-Stem, AFM, Evry Cedex 91030, France, [4]Centre de Génétique Moléculaire, UPR3404, CNRS, 1 avenue de la Terrasse, Gif sur Yvette 91198, France, [5]UMR S 787/INSERM/UPMC-Institut de Myologie, Paris Cedex 13 75634, France and [6]Département Pathologie et Immunologie, CMU, Centre Médicale Universitaire, 1 Rue Michel Servet, Genève 4, Suisse 1206, Switzerland

Received May 27, 2013; Revised July 16, 2013; Accepted July 29, 2013

Myotonic dystrophy type 1 (DM1) is an RNA-mediated disorder caused by a non-coding CTG repeat expansion that, in particular, provokes functional alteration of CUG-binding proteins. As a consequence, several genes with misregulated alternative splicing have been linked to clinical symptoms. In our search for additional molecular mechanisms that would trigger functional defects in DM1, we took advantage of mutant gene-carrying human embryonic stem cell lines to identify differentially expressed genes. Among the different genes found to be misregulated by DM1 mutation, one strongly downregulated gene encodes a transcription factor, ZNF37A. In this paper, we show that this defect in expression, which derives from a loss of RNA stability, is controlled by the RNA-binding protein, CUGBP1, and is associated with impaired myogenesis—a functional defect reminiscent of that observed in DM1. Loss of the ZNF37A protein results in changes in the expression of the subunit α1 of the receptor for the interleukin 13. This suggests that the pathological molecular mechanisms linking ZNF37A and myogenesis may involve the signaling pathway that is known to promote myoblast recruitment during development and regeneration.

INTRODUCTION

Myotonic dystrophy type 1 (DM1), the most common form of adult-onset muscular dystrophy, is caused by an abnormal CTG repeat expansion in the 3′ UTR (untranslated region) of the gene encoding a protein kinase (DMPK). This disease has a peculiar molecular basis because most of the clinical symptoms are not directly due to a defect in the function of the mutant DMPK gene (1,2). Instead, abnormalities are introduced in the processing of a variety of genes by an indirectly triggered defective activity of proteins involved in mRNA processing; this is the result of the presence of the mutant DMPK RNA in the cell nucleus (3). The identification of RNA-binding proteins bound to the abnormal CUG repeat expansion indicated an RNA gain-of-function model for DM1. Indeed, a number of changes in tissue-specific patterns of gene alternative splicing have been shown to contribute to the specific symptoms in DM1 patients (3,4).

In addition to these mechanisms, or as a secondary consequence of abnormal splicing in a signaling cascade, more recent studies have highlighted the existence of gene expression alterations in DM1 cells. Using differential transcriptomics, we specifically identified 15 genes that exhibited up- or downregulation in cells differentiated from stem cell lines derived from human embryos characterized as carrying the DM1 gene in a preimplantation genetic diagnosis (PGD) procedure (5,6). How

*To whom correspondence should be addressed. Email: cmartinat@istem.genethon.fr

such changes in gene expression may contribute to the disease phenotype remains to be established. Within this framework, ZNF37A—one of the most severely downregulated genes—particularly attracted our attention because it is a potential transcription factor. Modification of expression of transcription factors has been described in DM1 and may provide a powerful explanation for broad gene expression changes. This has been demonstrated for the abnormal heart Nkx2.5 induction in a DM1 mouse model (7,8). These findings also highlight the notion that the requirement for transcription factors in different tissues expressing the mutation may account for the multisystemic nature of DM1.

In the general framework of our search for new pathological mechanisms of DM1, we began with the identification of the expression defect of ZNF37A and subsequently explored its role in the DM1 pathophysiology. Derivatives of human ES cell lines were used in this study because they provide the dual advantage of the production of an unlimited number of cells, as a result of their indefinite capacity for self-renewal, and their ability to differentiate into homogenous cell populations of discrete phenotypes (9). As a complement to such studies, PGD permits the precise characterization of the genomic defect of the cell lines.

Our study reveals that the altered expression of the Krab-domain, zinc-finger transcriptional repressor factor ZNF37A bears functional consequences in myogenesis. The myogenic function of ZNF37A may be related to its transcriptional effect on IL13RA1—the expression of which was also altered in our original transcriptomic analysis (5)—because it is a subunit for the receptor to the myoblast recruitment factor interleukin 13 (IL13).

RESULTS

ZNF37A expression is specifically altered in cells with DM1 mutation

In our original transcriptomic analysis of cells differentiated from stem cell lines derived from embryos carrying a DM1 gene (data available at GEO Data Bank; accession number GSE7214, http://www.ncbi.nlm.nih.gov/geo/query/acc.cgi?acc=GSE7214), *ZNF37A* was found highly downregulated in human embryonic stem cells (hESCs), hESCs-derived mesenchymal stem cells (MSCs) and hESCs-derived neural stem cells (NSCs) (5). As previously shown, hES-derived MSCs are characterized by expression, at near homogeneity, of CD29 (β1-integrin), CD44 (H-CAM), CD73, CD105 and CD166, and are able to differentiate along osteogenic and adipogenic lineages when grown in appropriate conditions (10). The two DM1 hESCs, VUB03_DM and VUB24_DM, carry ∼1000 and 3000 CTG triplet repeats, respectively, and their differentiation into NSCs and MSCs does not affect the size of the CTG triplet repeats (5). *ZNF37A* gene encodes a zinc-finger protein that exhibits all the characteristics of the Krab-containing zinc-finger protein family. This gene belongs to a cluster of genes encoding members of that family, which is located in the pericentromeric region of the chromosome 10p11.2-10q11.2 (Fig. 1A). Specific down expression of *ZNF37A* was confirmed by quantitative reverse transcription-PCR (Fig. 1B; Supplementary Material, Fig. S1) and *in situ* hybridization (Supplementary Material, Fig. S1B). At the protein level, western blot and immunofluorescence analysis (Fig. 1D–F) also showed that ZNF37A expression was decreased in DM1 hES-derived MSCs, whereas the protein could be easily detected in the nucleus of control wild-type cells. Similarly, a strong gene expression defect was also observed both in skeletal muscle cell and brain tissue samples from DM1 patients (Fig. 1G–F).

DM1 affects ZNF37A expression by means of CUGBP1 control of its mRNA stability

Molecular mechanisms linking this defect with DM1 were explored by analyzing the hypothesis that the stability of ZNF37A mRNA was compromised in diseased cells. Indeed, measurement of the stability of transcripts following inhibition of the transcription with Actinomycin D indicated a specific instability of ZNF37A mRNA in DM1 hES-derived MSCs as compared to control cells, whereas no effect of the treatment was observed on ZNF33A and ZNF37B, two other genes of the same family that belong to the same chromosomal cluster (Figs 1A and 2A; Supplementary Material, Fig. S2A).

A part of the 5′ UTR region of the ZNF37A mRNA contains several UG-rich motifs (Fig. 2B); similar motifs have been shown to be CUGBP1-binding sites (11). This observation, together with the fact that CUGBP1 function is known to be aberrant in DM1, suggested a link between CUGBP1 and the ZNF37A mRNA instability. To test this hypothesis, a luciferase reporter plasmid was used in which this part of the 5′UTR_ZNF37A had been cloned upstream of the luciferase gene under a CMV promoter (Fig. 2B). Transient transfection of this construct in DM1 hES-derived MSCs resulted in a statistically significant decrease in luciferase expression as compared with control cells, whereas no difference was observed in transfection efficiency (Fig. 2C; Supplementary Material, Fig. S2B). Similar results were obtained in wild-type HEK 293 cells after co-transfection of the luciferase construct together with a plasmid expressing a DMPK minigene that contains an abnormally long stretch of 960 interrupted CUG repeats (Fig. 2F; Supplementary Material, Fig. S2C and D) (12). The overexpression of CUGBP1 resulted in a similar reduction in luciferase expression, whereas the overexpression of MBNL1, another RNA-binding protein known to be affected in DM1, had no effect (Fig. 2F). Whether CUGBP1 controlled the expression of ZNF37A by means of direct binding to RNA was determined using gel shift retardation assays. Thus, four different RNA fragments derived from the ZNF37A 5′ UTR were incubated with increasing amounts of recombinant CUGBP1 protein and the complexes were separated on a native polyacrylamide gel. CUGBP1 seemed to bind predominantly two different fragments (fragment 2 and fragment 4) of the 5′ UTR of ZNF37A (Fig. 2D and E). The deletion of a region that contained CUGBP1-binding motifs in 5′UTR_ZNF37A-luc construct (Delta A) resulted in a loss of effect of the DMPK minigene containing 960 CUG repeats as well as a loss of effect of CUGBP1. In contrast, the deletion of a region (Delta B) that does not contain putative CUGBP1-binding motifs did not affect the response of the 5′UTR_ZNF37A-luc construct (Fig. 2F). However, we cannot exclude, as it was recently suggested by different studies, that the RNA secondary structure may facilitate CUGBP1 binding by bringing into close proximity UGU sequences dispersed throughout the region (13,14). Thus, the identification of CUGBP1-binding sites might not be clearly as simple as

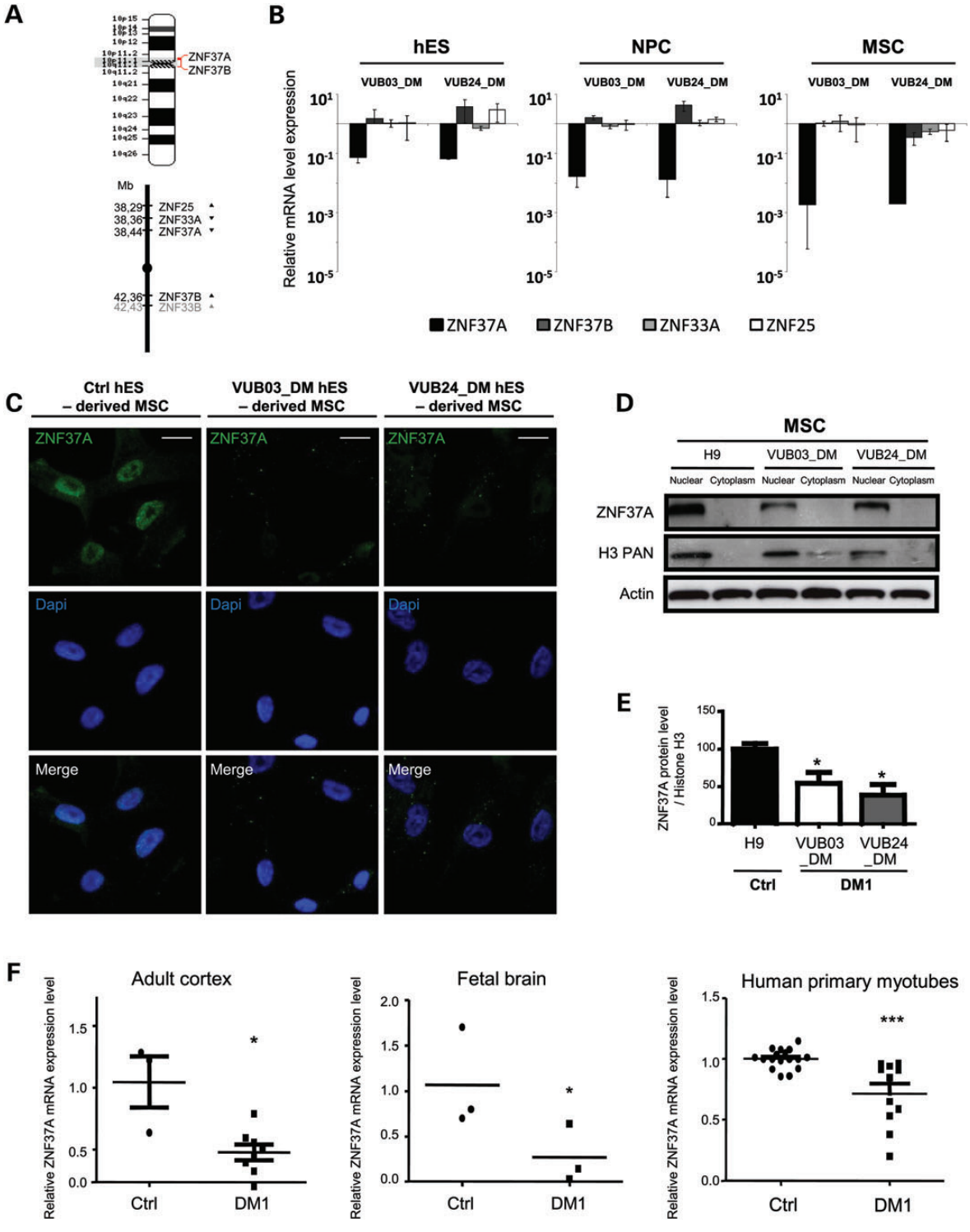

Figure 1. *ZNF37A* is a transcription factor specifically downregulated in DM1 hESC, its progeny and patients biopsies. (**A**) *ZNF37A* belongs to a gene cluster localized on the pericentromeric part of the chromosome 10. (**B**) Quantitative real-time RT–PCR analysis of *ZNF37A*, *ZNF37B*, *ZNF33A* and *ZNF25* expression in the two DM1 hES cell lines (VUB03_DM and VUB24_DM) and in their differentiated derivatives (NPC and MSC). Data ($n = 3$) are presented as values of the control VUB01 and were analyzed with ANOVA followed by Student's *t*-test.$^{*}P \leq 0.005$. (**C**) ZNF37A nuclear localization by immunostaining on control hES-derived MSCs (H9) compared with DM1 hES-derived MSCs (VUB03_DM and VUB24_DM). Nuclei were stained with Dapi. Bar scale = 20 μm. (**D**) Western blot analysis of ZNF37A expression in DM1 hES-derived MSCs (VUB03_DM and VUB24_DM) in comparison with the wild-type cell line (H9). H3 PAN was used as a nuclear positive fraction control; actin was used as a loading control. (**E**) Quantification of ZNF37A protein level after western blot by using ImageJ software. Similar results were obtained with 10, 5, 2.5 and 1.25 μg of proteins loaded. Data ($n = 3$) were normalized with Histine H3 level and were analyzed with a *t*-test ANOVA, $^{*}P < 0.0001$. (**F**) Quantitative real-time RT–PCR analysis of *ZNF37A* expression in cerebral tissues from DM1 patients as well as in primary skeletal muscle cells isolated from DM1 patients (results were normalized with the average of control samples). Data are presented as scatter dot plots (line at mean) and were analyzed with the *t*-test, $^{*}P < 0.05$.

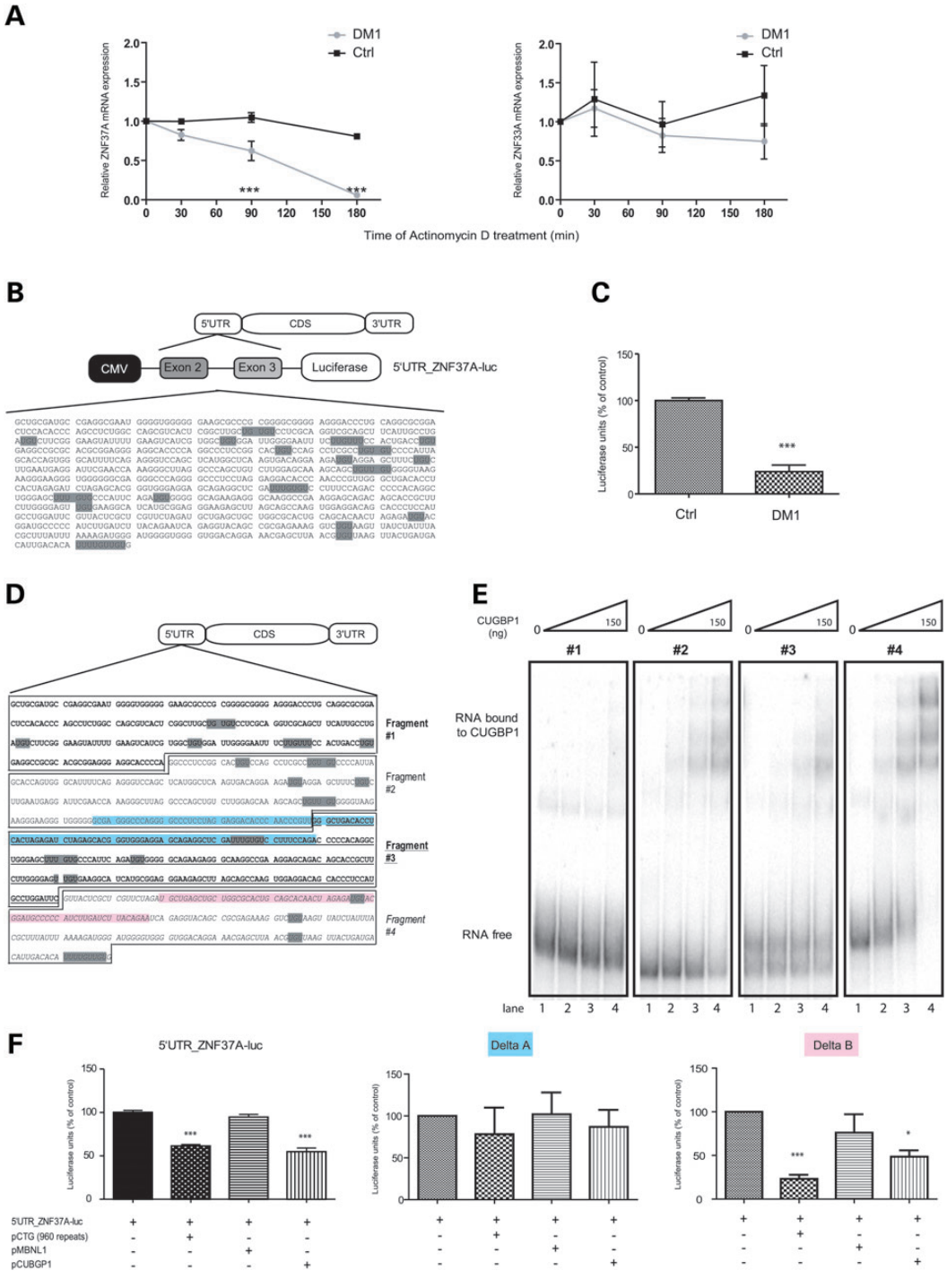

Figure 2. ZNF37A misexpression is due to mRNA instability modulated by CUGBP1. (**A**) Quantitative real-time RT–PCR of *ZNF37A* in DM1 (VUB03_DM) hES-derived MSCs treated with actinomycin D compared with control cells (H9). Data are presented as the mean ± SEM ($n = 3$) and were analyzed with the *t*-test ANOVA, $^{***}P < 0.001$. (**B**) Schematic representation of 5′UTR_ZNF37A-luc constructs containing the ZNF37A-5′ UTR potential RNA-binding protein motifs (highlight in gray) between the luciferase gene and under the control of CMV promoter. (**C**) Luciferase expression of 5′UTR_ZNF37A-luc constructs after co-transfection with a GFP expressing plasmid in DM1 (VUB03_DM) hES-derived MSCs, when compared with controls. Normalization was achieved by adjusting to the number of GFP positive cells. Data are presented as the mean ± SEM ($n = 3$) and were analyzed with the *t*-test (ANOVA), $^{*}P < 0.05$. (**D**) Schematic design of 300 nt sequences in UGU rich region of ZNF37A 5′ UTR named #1, #2, #3, #4. UGU motifs are highlighted in gray. Deletion of mutant Delta A is underlined in blue and mutant Delta B is underlined in pink. (**E**) Gel shift assay of CUGBP1 binding to the four different regions of ZNF37A 5′ UTR. Increasing quantities of CUGBP1 protein were incubated with the different ZNF37A 5′ UTR regions (lane 1: 0 ng; lane 2: 37.5 ng; lane 3: 75 ng; lane 4: 150 ng). (**F**) Luciferase expression of 5′UTR_ZNF37A-luc, Delta A and Delta B constructs in HEK293 cells, cotransfected with the GFP expressing plasmid and the RNA-binding protein CUGBP1, MBNL1 and DMPK 3′ UTR containing 960 CUG interrupted repeats (pCTG). Normalization was achieved by adjusting to the number of GFP positive cells. Data are presented as the mean ± SEM ($n = 3$) and were analyzed with the *t*-test (ANOVA), $^{**}P < 0.001$.

pinpointing extensive UG-rich regions and further investigation will be necessary to enable accurate prediction of CUGBP1 targets.

An alternative hypothesis for explaining the defect in ZNF37A expression was the presence of a putative alternative splice site in the 5′ UTR of ZNF37A, which may alter the stability of the ZNF37A transcript. To test this hypothesis, the construct was inserted upstream of the luciferase gene in an inverse position. Similar results were obtained regardless of the sense of the insertion (Supplementary Material, Fig. S2E), thus ruling out the presence of an alternative splicing defect. This was further confirmed by the lack of effect of either CUGBP1 overexpression or the introduction of the construct carrying 960 CUG repeats on the alternative splicing of this region (Supplementary Material, Fig. S2F). Altogether, these results suggest that DM1-specific ZNF37A down expression is linked to a CUGBP1-dependent mRNA destabilization mechanism.

ZNF37A down expression results in altered myogenesis that may involve the IL13 receptor α1 subunit

In an attempt to identify a functional link between the defect in ZNF37A expression and DM1, the former's role was explored. Judging from its nuclear subcellular localization (Fig. 1D–E) and its sequence analysis, ZNF37A exhibits all the characteristics of Krab-containing zinc-finger proteins, which generally function as transcriptional repressors (15). Accordingly, co-immunoprecipitation on the nuclear fraction of control hES-derived MSCs demonstrated a direct interaction between ZNF37A and Kap1, a common co-repressor of Krab-domain transcription factors (Supplementary Material, Fig. S3A).

It was, therefore, postulated that ZNF37A down expression in DM1 cells might induce upregulation of its target genes in the same cells. Among the seven candidates found to be upregulated in our original study (5), the α1 chain of the receptor to IL13 (IL13RA1) was especially appealing because its expression level was inversely correlated to that of *ZNF37A* not only in mutant hES cells and derivatives at all stages and types of differentiation but also in DM1 patients' myotubes samples (Fig. 3A and B; Supplementary Material, Fig. S3B). The knockdown of *ZNF37A* expression by specific siRNA in wild-type H9 hES-derived MSCs led to an increased expression of *IL13RA1*, confirming that ZNF37A negatively controls the expression of *IL13RA1* (Fig. 3C). As a control of the specificity of those effects, *ZNF37A*-directed siRNA had no effect on the expression level of eIF2S3, another gene upregulated in the mutant cells (Supplementary Material, Fig. S3C). Chromatin immunoprecipitation directed against ZNF37A, followed by a quantitative PCR analysis with primers covering the entire *IL13RA1* promoter, revealed a potential-binding site for ZNF37A that did not exist in the promoter region of eIF2S3 (Fig. 3D; Supplementary Material, Fig. S3D and E).

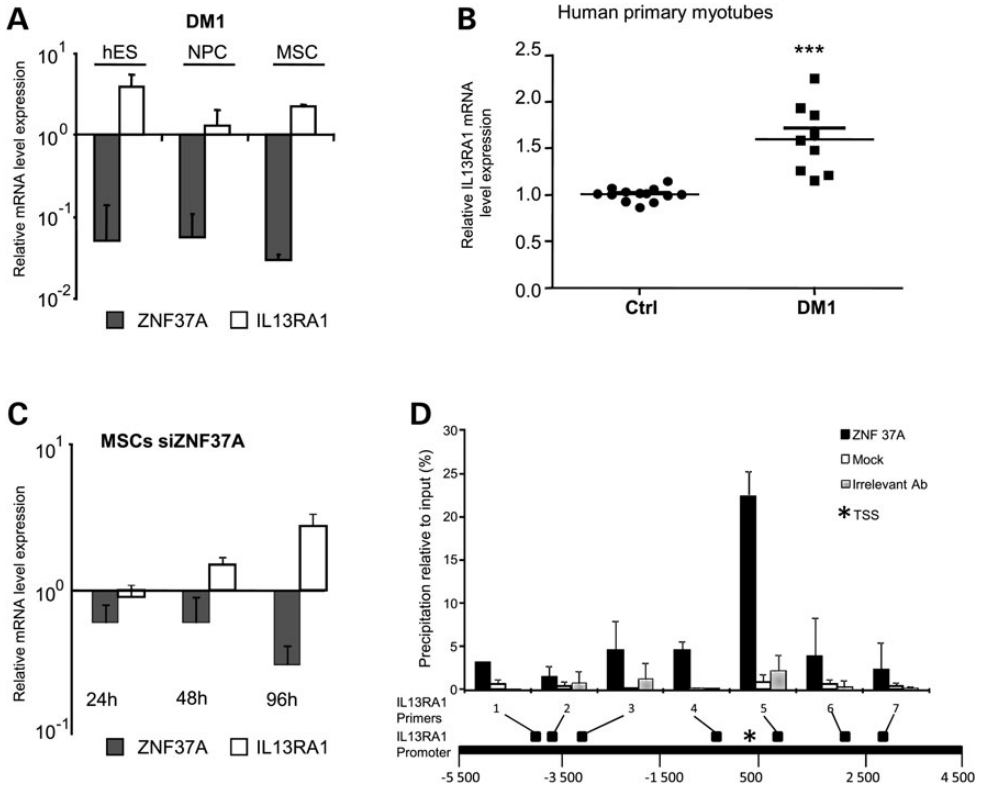

Figure 3. ZNF37A modulates IL13RA1 expression. (**A**) Quantitative real-time RT–PCR of *ZNF37A* and *IL13RA* expression in undifferentiated DM1 (VUB03_DM) hES cell lines and in their differentiated derivatives NPC and MSC). (**B**) Quantitative real-time RT–PCR of *IL13RA* expression in primary cultures of myotubes isolated from DM1 patients (results were normalized with the average of control samples). Data are presented as scatter dot plot (line at mean) and were analyzed with the *t*-test, $^{*}P < 0.05$. (**C**) Quantitative real-time RT–PCR of *ZNF37A* and *IL13RA1* expression after siRNA-induced knock down in controls (H9) hES-derived MSCs. (**D**) Chromatin immunoprecipitation of ZNF37A on *IL13RA1* promoter. Different primers have been designed to cover a large region surrounding the transcription start site (TSS) and their localization is schematically indicated. Data are expressed as percent precipitation relative to input (mean ± SEM, $n = 4$).

IL13RA1 is part of the common receptor for IL4 and IL13, two cytokines that participate to the recruitment of myoblasts and promote myogenic fusion (16,17). Function of ZNF37A was, therefore, evaluated on muscle cell differentiation. Control human primary myoblasts transfected either with one of two different siRNA against ZNF37A (Supplementary Material, Fig. S4A and B) or with control siRNA were differentiated into myotubes. Down expression of ZNF37A did not affect the generation of myotubes, as determined by the detection of myosin heavy chain (MF20 positive cells). In contrast, a defect in the number of nuclei per MF20 positive cells was observed, similar to that observed in human primary myoblasts derived from DM1 patients (Fig. 4; Supplementary Material, Fig. S4C). These results suggested that the down expression of ZNF37A might not affect the differentiation process, but instead plays a role in the myoblast fusion at a specific stage of myogenesis

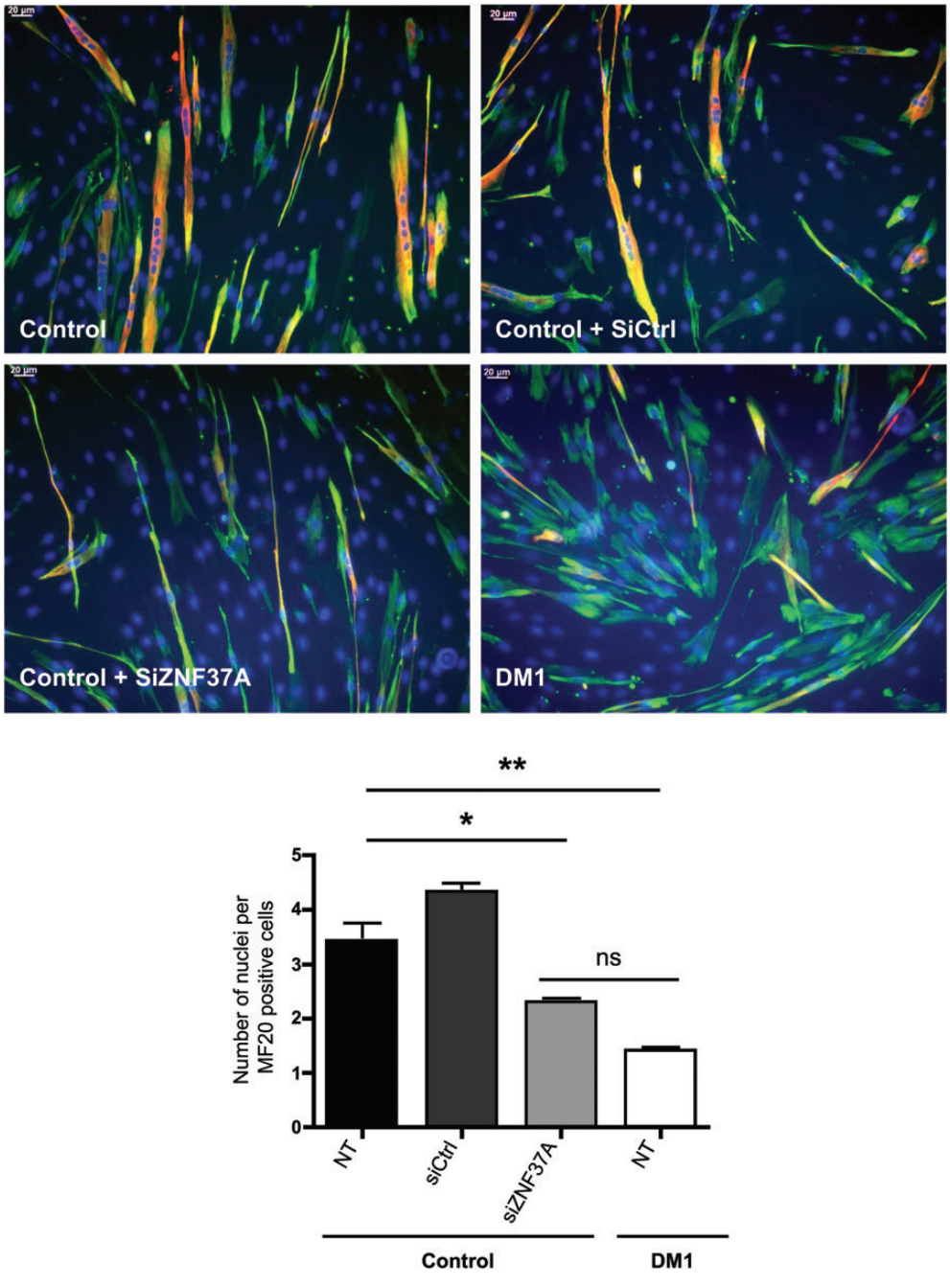

Figure 4. Down expression of ZNF37A affects myogenic differentiation *in vitro*. Detection of myogenic markers by immunostaining 6 days after specific ZNF37A siRNA transient transfection in control myoblasts. Desmin detects muscle cells (green); MF20 detects differentiated myoblasts (red) and Dapi (blue) labels nuclei. Scale bar = 50 μm. Quantification of the myogenic impairment is measured by the number of nuclei per MF20 positive cells. A total of ~1000 MF20 was counted for each condition. Data are presented as mean ± SEM ($n = 3$) and were analyzed with a 'Bonferroni's multiple comparison test' (one-way ANOVA), ns: no statistical difference, $^{*}P < 0.05$, $^{**}P < 0.001$.

after the initial formation of a myotube. No statistical difference was observed between DM1 myotubes and siZNF37A-treated cells, suggesting that the down expression of ZNF37A led to a similar phenotype to that observed in DM1 cells. This action window of ZNF37A on myogenesis could be correlated with the one of the cytokines IL13 and IL4, which reinforced the hypothesis of a mechanistic action of ZNF37A via IL13RA1. To validate this point, the effect of IL4/IL13 treatment on myogenesis was compared between DM1 cell cultures and wild-type cells treated to knock down the expression of ZNF37A. In the controls, IL4/IL13 treatment increased the ability of wild-type myoblasts to mature into multinucleated myotubes. In sharp contrast, no similar effect of the treatment was observed in either DM1 myoblasts or wild-type myotubes after knocking down the expression of ZNF37A using specific siRNAs (Fig. 5) which thus establishes the contribution of ZNF37A to the myogenic effect of IL4/IL13.

DISCUSSION

The main finding of this study is the demonstration that, in cells carrying the DM1 mutation, the observed decreased expression of the transcription factor ZNF37A bears functional consequences for myogenesis. These results from a defect in IL4/IL13 signaling that may involve alteration of expression of the IL13RA1 receptor subunit. At the molecular level, the DM1 mutation most likely affects ZNF37A expression via a mechanism that involves abnormal control of its mRNA stability by the RNA-binding Protein CUGBP1.

The currently accepted pathological model of DM1 holds that manifestations result from alteration of two main proteins involved in pre-mRNA splicing, namely MBNL1, which is sequestered in the nucleus due to its association with the repeat-containing mRNA (18), and CUGBP1, which is overexpressed and hyperphosphorylated in the nucleus of DM1 cells (19). Recent studies have shown that not all DM1 pathological mechanisms can be explained by altered alternative RNA splicing. By characterizing affected genes in a DM1 transgenic mouse model expressing 250 CUG repeats in 3′ UTR of the skeletal actin mRNA, Osborne *et al*. have shown that RNA containing (CUG) expansions interfere at both transcriptional and posttranscriptional levels (20). Similarly, the misexpression of CUGBP1 contributes to the alteration in muscle development in DM1 by affecting the translation efficiency of p21 via binding to a GC-rich sequence located within the 5′ region of p21 mRNA (21,22). CUGBP1 also acts as an mRNA stabilizing factor associated with short-lived mRNAs (23) and contributes to muscle wasting in DM1 by affecting the decay of TNF mRNA in DM1 muscle cells (13). Collectively, these observations and our results support the conclusion that the function of CUGBP1 on the turnover of mRNA has a more extensive impact on DM1 pathogenesis than previously thought.

The involvement of a zinc-finger transcription factor in DM1 requires a comparison with DM2, a myotonic dystrophy disorder characterized by CCUG mRNA expansions (24) in *ZNF9*, another member of zinc-finger transcription family. The clinical analogies between DM1 and DM2 have led to the suggestion of a common trans-acting mechanism with depletion of similar transcription factors (25). The observation that haploinsufficiency for *Znf9* is associated with multiorgan abnormalities resembling myotonic dystrophy reinforces this notion (26,27). It is therefore tempting to postulate that a common requirement for transcription factors in tissues expressing the mutant DMPK may be partially responsible for some of the multisystemic symptomatology of DM1 (e.g. myotonia, myopathy, insulin resistance, cognitive impairment). To address this issue, it would be interesting to undertake a systematic search for target genes impacted by the loss of *ZNF37A* expression in DM1.

The DM1 mutation interferes with myogenesis, but the exact mechanism of this phenomenon has not yet been clarified (3,28). IL13 and IL4 can be considered as interesting candidates because of their role in myoblast fusion during muscle development and regeneration (16,17,29). It was, therefore, particularly interesting to observe that ZNF37A, which interferes with myogenesis when defective, was found to modulate the expression of *IL13RA1.* This gene encodes a receptor subunit that combines with IL4RA to form the heterodimeric receptor for the IL4 and IL13 cytokines (30). *IL13RA1* expression also increases soon after muscle injury, suggesting that this receptor plays a role in muscle regeneration (31). Increased expression of *IL13RA1* in DM1 cells as a consequence of a loss of expression of *ZNF37A* may, therefore, bear some significance for myogenesis and/or regeneration (32–35). Consistent with this, DM1 differentiated myoblasts did not respond to IL13/IL4 treatment in an *in vitro* model of myogenic fusion as control cells did.

However, it has been shown that IL-4 and IL-13 could share the redundant ability to recruit mononucleated cells for fusion but not toward the same cell populations: IL-4 being responsible for the ‘normal’ myoblast fusion into nascent myotubes during myogenic differentiation, and IL-13 for additional recruitment of reserve cells during skeletal muscle hypertrophy that may prevent the loss of muscle mass (16,17,29). Therefore, it will be interesting to determine the exact function of IL4 and IL13 in the DM1 phenotype observed.

Most previous analyses of DM1 pathological mechanisms attempted to associate clinical symptoms and alteration of the processing of specific candidate proteins. These hypothesis-driven studies unavoidably ignored genes that could not be directly linked to identified symptoms. We have begun to provide a complementary list of genes that appear to be specifically modified by the presence of DM1 mutation by combining the use of DM1-mutant hES cells-derived progenies and global gene expression profiling. Although validation of the exact mechanisms by which DM1 affects these genes has yet to be provided and the effect of their abnormal expression on cell metabolism still has to be defined, these genes are candidates for new pathological pathways associated with DM1. We previously demonstrated that this approach could be used to identify new physiopathological mechanisms implicated in the neuritogenesis and synaptogenesis of motoneurons (5). The present study confirms the usefulness of such a resource-driven approach based on gene-carrying pluripotent stem cell lines. This study also highlights the potential offered by the use of disease-specific human pluripotent stem cells to decipher physiopathological mechanisms in a large spectrum of cell types, and therefore points out the added value of this approach for multisystemic diseases.

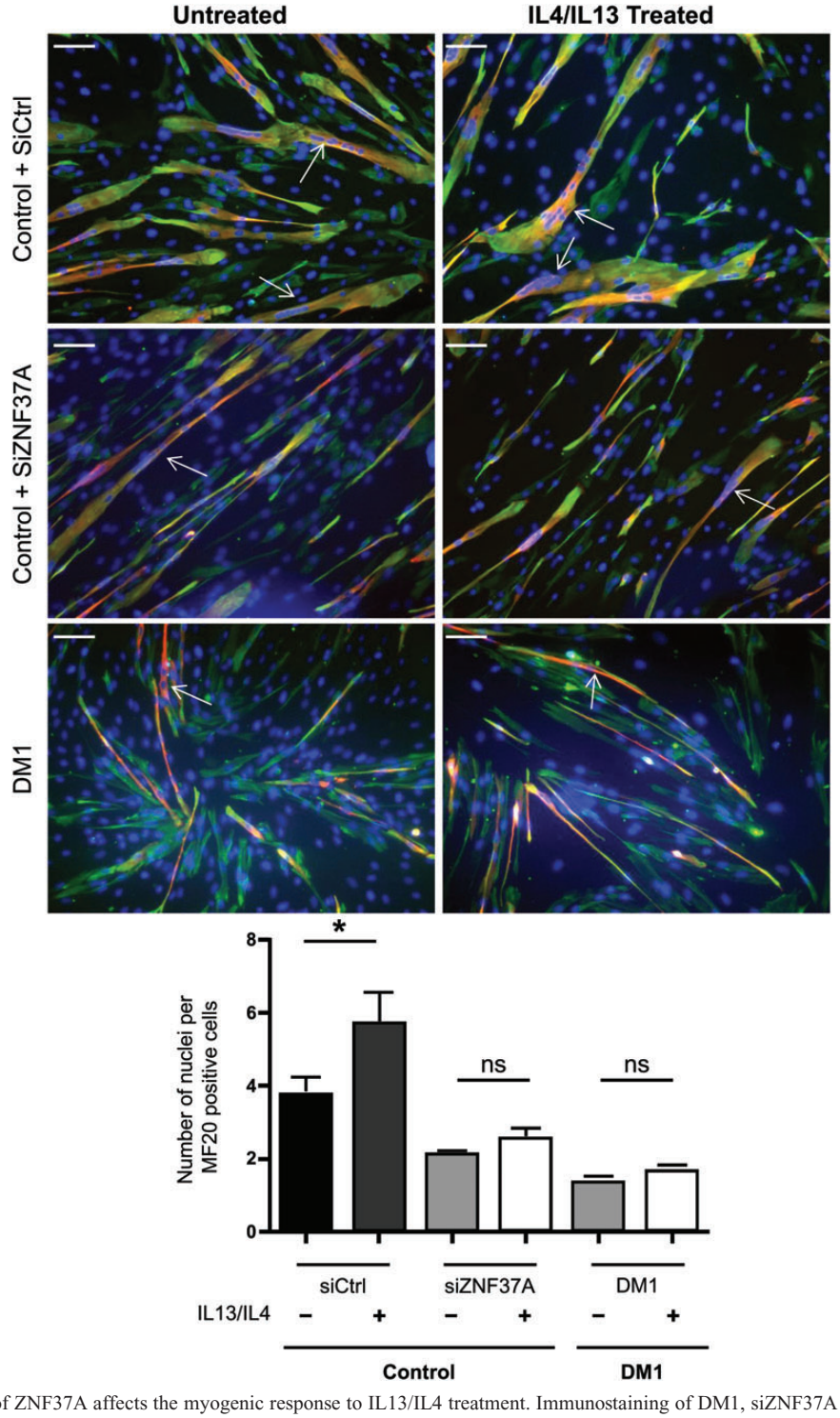

Figure 5. Down expression of ZNF37A affects the myogenic response to IL13/IL4 treatment. Immunostaining of DM1, siZNF37A transfected or untransfected control myoblasts treated with IL13/IL4 (50/50 ng/ml) on Day 6 of differentiation. Desmin detects muscle cells (green); MF20 detects differentiated myoblasts (red) and Dapi (blue) labels nuclei. White arrows indicate examples of polynucleated MF20 positive cells. Scale bar = 50 μm. Quantification of the myogenic impairment was measured by the number of nuclei per MF20 positive cells. A total of ~1000 MF20 was counted for each condition. Data are presented as mean ± SEM ($n = 3$) and were analyzed with the 'Bonferroni's multiple comparison test' (one-way ANOVA), $^{*}P < 0.05$. NT: non-transfected.

MATERIALS AND METHODS

Cell culture

Mutants hES cell line (VUB03_DM, XX, passages p70–p90; and VUB24_DM; XX, passages p30–40, derived in AZ-VUB) and wild-type human ES cells (H9, XX, passages 40–60; WiCell Research Institute; VUB01, XY, passages p80–90) were maintained as previously described (36).

Control and DM1 myoblasts were cultured in D-MEM/F-12 medium (Invitrogen) supplemented with 20% SVF (Eurobio)

and 0.1% of penicillin–streptomycin (Gibco). For differentiation, cells were transferred to 2% SVF D-MEM/F-12 medium for 6 days.

Neural and mesodermal differentiation were achieved using established methods (5,10,37). Briefly, mesodermal stem cells were obtained after plating hES cells onto gelatin-coated plates with medium containing 20% of fetal bovine serum for 21 days. The purity of the mesenchymal cultures was validated by FACS analysis for different markers such as CD73 (5,10). hES cell lines were differentiated into neural precursor cells by using a co-culture with MS5 stromal cells. After 2–3 weeks of culture, neural precursor cells appear as neural rosette structures. Neural precursor cells were FACS-sorted on the basis of NCAM expression.

Control and DM1 myoblasts with >2000 repeats (kindly provided by Dr. D. Furling) were isolated from quadriceps muscles biopsies obtained from the Myobank in accordance with the French legislation on ethical rules. The fetal brain RNA (kindly provided by Dr. G. Gourdon, Inserm U781) was obtained from fetuses aged from 12 to 25 amenorrhea weeks. DM1 samples were affected to different degrees (97–1500 CTG repeats). The adult brain RNA samples (kindly provided by Dr. M. Gomez-Pereira, Inserm U781) were obtained from cortical biopsies of adult forms of DM1 and contained different sizes of CTG expansion ranging from 200 to 1000.

Real-time reverse transcriptase polymerase chain reaction and Agilent DNA chips analysis

Total RNA from cells was isolated using the 'RNeasy Mini Protocol' (Qiagen). cDNA was synthesized by using SuperScript III (Invitrogen). Quantitative real-time reverse transcriptase–polymerase chain reaction (RT–PCR) was optimized to determine the linear amplification range by using a Chromo4 Real-Time System (Bio-Rad) with Syber Green PCR Master Mix (Applied Biosystems). For Agilent Chips analysis, PCR products were quantified using the DNA 1000 Kit for the Agilent 2100 Bioanalyzer (Agilent Technologies, Palo Alto, France) according to the manufacturer's protocol. Primers are listed in Supplementary Material, Table S1.

Actinomycin treatment

hES-derived MSCs control (H9) and DM1 (VUB03_DM) were plated at 5×10^4 cells per well (70–80% confluency in 24-well plate) and were treated with 5 μg/ml of Actinomycin (Sigma) during 30, 90 and 180 min. Total RNA from cells was isolated as described above and quantitative real-time RT–PCR was performed.

Luciferase assays

5′UTR_ZNF37A-luc plasmid was obtained by PCR using specific primers amplifying DNA intron 1 to intron 3. The PCR product was purified and cloned in pGL4.82 (Promega) modified with CMV promoter. HEK293 cells were plated at 2.5×10^4 cells/cm^2 in 96-well plate in Alpha MEM medium supplemented with 10% SVF (Hyclone) and 1% Glutamax, 1% non-essential amino acids and 1% penicillin–streptomycin (Gibco). Twenty-four hours after plating, the cells were co-transfected with 100 ng of the 5′UTR_ZNF37A-luc, 100 ng of Delta A or 100 ng of Delta B, 250 ng of the pGFP (Lonza) and 250 ng of pCTG (960 interrupted repeats) or 100 ng of pCUGBP1 or 100 ng of pMBNL1 plasmids in OptiMEM medium using Lipofectamine™ LTX PlusReagent (Invitrogen). Forty-eight hours after transfection, the luciferase substrate was applied using Enduren™ Live Cell Substrate (Promega). Luminescence reading was performed using Analyst GT (Molecular Devices). For cell normalization, CellTiterGlo® Luminescent Cell Viability Assay (Promega) was used.

Transient siRNA knockdown

The sequences targeted by chemically synthesized siRNAs in transient knockdown experiments were as follows: Hs_ZNF37A_7 HP siRNA (Qiagen), Hs_ZNF37A_9 HP siRNA (Qiagen) and Silencer® Negative Control siRNA (Ambion, Applied Biosystems). MSCs were plated at 5×10^4 cells per well (70–80% confluency in 24-well plate) and were transfected the following day with 10–40 nmol siRNA in OptiMEM medium by using LipoRNAiMax (Invitrogen).

Myoblasts were plated at 8×10^4 cells per well in 12-well plate. The following day, they were transfected with 10 pmol siRNA in OptiMEM medium by using Lipofectamine 2000 (Invitrogen) in differentiated medium. Forty-eight hours after transfection, RNA was isolated and quantitative real-time RT–PCR was performed as described above to check the specific ZNF37A down expression.

Immunocytochemistry

Cultured cells were fixed in 4% paraformaldehyde in PBS and were incubated with the monoclonal antibody against ZNF37A (R&D System, 1/500) at 4°C for 12 h. Appropriate FITC-labeled secondary antibodies (Jackson ImmunoResearch) were used. For myogenic characterization, the cells were fixed in 4% paraformaldehyde in PBS and were incubated with the monoclonal antibody MF20 (DSHB, 1/200) and Desmin (1/25 R&D System) at RT for 2 h. Then the cells were incubated with Monoclonal Cy3 and Cy2 and Dapi at RT for 2 h. Images were captured using a Zeiss fluorescent microscope.

Chromatin immunoprecipitation

Chromatin immunoprecipitation analyses were carried out as described (38,39). Briefly, genomic DNA and proteins were cross-linked by formaldehyde (1% final) and quenched with glycine 1 M. Cells were sonicated eight times to generate 100–1000 bp DNA fragments. Before addition of antibody, 100 μl of lysate was saved as the input sample. Either anti-acetyl H3, CT, pan A3S (Millipore, 5 μg), monoclonal anti-ZNF37A (R&D System, 5 μg), monoclonal anti-Isl2 or MAP2 (DSBH Bank, 5 μg) was incubated with lysates overnight at 4°C. Immune complexes were purified using Dynead beads (Invitrogen) and eluted at 100°C for 10 min. DNA was extracted using purification columns (Nalgene) and quantitative PCR was carried out and analyzed as described in (40) using the primers described in Supplementary Material, Table S1.

In vitro transcription and gel shift assay

RNAs for gel shift experiments were transcribed using a cap analog and SP6 polymerase in the presence of α-32P-[UTP]. RNA mobility shift assays were performed with increasing concentrations of recombinant CUGBP1 as described previously (41). Recombinant proteins were diluted in buffer D containing 0.5 mg/ml bovine serum albumin. The reaction was incubated for 15 min at 30°C, and the protein complexes were resolved by electrophoresis on a 6% non-denaturing polyacrylamide gel (39/1), 0.5× TBE. RNA bands were quantified using a PhosphorImager (Molecular Dynamics)

Co-immunoprecipitation and western blot analysis

Co-immunoprecipitation and western blot analyses were performed as previously described (42). Briefly, proteins were extracted with RIPA buffer (Invitrogen) and were quantified using a BCA protein assay kit (Pierce). For co-immunoprecipitation, 100 μg of proteins were incubated overnight at 4°C with 10 μg of antibodies against either ZNF37A (Abnova) or Kap1 (Abnova). Precipitation were performed with Dynabeads® Protein A (LifeTech®) according to manufacturer's protocol. For western blot, 15 μg of proteins were loaded on NuPAGE 4–12% Bis-Tris Gels (Invitrogen) and transferred onto a nitrocellulose membrane (Invitrogen). Primary antibodies for ZNF37A (1/500, Abnova), H3 PAN (1/1000, Millipore), β-Actin (1/100 000, Sigma), MBNL1 (1/7000, kindly provided by Dr. Furling) and CUGBP1 (1/1000, Santa Cruz Biotechnology) have been used. Western blot proteins were determined by using Novex®ECL Kit (LifeTech). For ZNF37A blots, nuclear and cytoplasm proteins were extracted using NE-PER Extraction Kit (Pierce).

IL13/IL4 treatment

Myoblasts were plated at 8×10^4 cells per well in 12-well plate. The following day, they were treated with 50 ng/ml of IL13 and IL4 (R&D System) in differentiation medium. The medium was changed after 4 days, and the cells were fixed on day 6.

Statistical analysis

The data were processed using Prism5.0c. Values are reported as means ± SEM. Comparisons between two groups were made with Student's *t*-test (ANOVA). For comparisons of more than two groups, 'Bonferroni's multiple comparison test' (one-way ANOVA) was performed.

SUPPLEMENTARY MATERIAL

Supplementary Material is available at *HMG* online.

ACKNOWLEDGEMENTS

We thank Gillian Butler-Brown and Vincent Mouly, UMR S 787 Paris, France and Jack Puymirat at CHUQ, Quebec, Canada for helpful discussions, Genevieve Gourdon INSERM U781, Paris, France for performing the CTG repeat analysis and the platform of Institut Curie, Paris for performing the DNA chip analysis, Nicolas Charlet, INSERM U596, Ullkirch, France for providing minigene plasmids, Karen Sermon, AZ-VUB Brussels for providing the DM1-mutant ES cell lines and Noel Buckley, King's London College, UK for chromatin immunoprecipitation analysis.

Conflict of Interest statement: None declared.

FUNDING

This work was supported in part by AFM (Association Française des Myopathes) and additional grants from MediCen (IngeCell program) and Genopole. M.G. has a fellowship from the French Ministry of Research and Higher Education. A.M. had a fellowship from the Regional Council Ile de France (Stem-Pôle).

REFERENCES

1. Machuca-Tzili, L., Brook, D. and Hilton-Jones, D. (2005) Clinical and molecular aspects of the myotonic dystrophies: a review. *Muscle Nerve*, **32**, 1–18.
2. Mahadevan, M., Tsilfidis, C., Sabourin, L., Shutler, G., Amemiya, C., Jansen, G., Neville, C., Narang, M., Barcelo, J., O'Hoy, K. *et al.* (1992) Myotonic dystrophy mutation: an unstable CTG repeat in the 3′ untranslated region of the gene. *Science*, **255**, 1253–1255.
3. Ranum, L.P. and Cooper, T.A. (2006) RNA-mediated neuromuscular disorders. *Annu. Rev. Neurosci.*, **29**, 259–277.
4. Wheeler, T.M. and Thornton, C.A. (2007) Myotonic dystrophy: RNA-mediated muscle disease. *Curr. Opin. Neurol.*, **20**, 572–576.
5. Marteyn, A., Maury, Y., Gauthier, M.M., Lecuyer, C., Vernet, R., Denis, J.A., Pietu, G., Peschanski, M. and Martinat, C. (2011) Mutant human embryonic stem cells reveal neurite and synapse formation defects in type 1 myotonic dystrophy. *Cell Stem Cell*, **8**, 434–444.
6. Mateizel, I., De Temmerman, N., Ullmann, U., Cauffman, G., Sermon, K., Van de Velde, H., De Rycke, M., Degreef, E., Devroey, P., Liebaers, I. *et al.* (2006) Derivation of human embryonic stem cell lines from embryos obtained after IVF and after PGD for monogenic disorders. *Hum. Reprod.*, **21**, 503–511.
7. Ebralidze, A., Wang, Y., Petkova, V., Ebralidse, K. and Junghans, R.P. (2004) RNA leaching of transcription factors disrupts transcription in myotonic dystrophy. *Science*, **303**, 383–387.
8. Yadava, R.S., Frenzel-McCardell, C.D., Yu, Q., Srinivasan, V., Tucker, A.L., Puymirat, J., Thornton, C.A., Prall, O.W., Harvey, R.P. and Mahadevan, M.S. (2008) RNA toxicity in myotonic muscular dystrophy induces NKX2–5 expression. *Nat. Genet.*, **40**, 61–68.
9. Maury, Y., Gauthier, M., Peschanski, M. and Martinat, C. (2012) Human pluripotent stem cells for disease modelling and drug screening. *Bioessays*, **34**, 61–71.
10. Denis, J.A., Rochon-Beaucourt, C., Champon, B. and Pietu, G. (2010) Global transcriptional profiling of neural and mesenchymal progenitors derived from human embryonic stem cells reveals alternative developmental signaling pathways. *Stem Cells Dev.*, **20**, 1395–1409.
11. Faustino, N.A. and Cooper, T.A. (2003) Pre-mRNA splicing and human disease. *Genes Dev.*, **17**, 419–437.
12. Philips, A.V., Timchenko, L.T. and Cooper, T.A. (1998) Disruption of splicing regulated by a CUG-binding protein in myotonic dystrophy. *Science*, **280**, 737–741.
13. Zhang, L., Lee, J., Wilusz, J. and Wilusz, C. (2008) The RNA-binding protein CUGBP1 regulates stability of tumor necrosis factor mRNA in muscle cells. *J. Biol. Chem.*, **283**, 22457–22463.
14. Teplova, M., Song, J., Gaw, H.Y., Teplov, A. and Patel, D.J. (2010) Structural insights into RNA recognition by the alternate-splicing regulator CUG-binding protein 1. *Structure*, **18**, 1364–1377.
15. Urrutia, R. (2003) KRAB-containing zinc-finger repressor proteins. *Genome Biol.*, **4**, 231.
16. Jacquemin, V., Butler-Browne, G.S., Furling, D. and Mouly, V. (2007) IL-13 mediates the recruitment of reserve cells for fusion during IGF-1-induced hypertrophy of human myotubes. *J. Cell Sci.*, **120**, 670–681.

17. Horsley, V., Jansen, K.M., Mills, S.T. and Pavlath, G.K. (2003) IL-4 acts as a myoblast recruitment factor during mammalian muscle growth. *Cell*, **113**, 483–494.
18. Mankodi, A., Urbinati, C.R., Yuan, Q.P., Moxley, R.T., Sansone, V., Krym, M., Henderson, D., Schalling, M., Swanson, M.S. and Thornton, C.A. (2001) Muscleblind localizes to nuclear foci of aberrant RNA in myotonic dystrophy types 1 and 2. *Hum. Mol. Genet.*, **10**, 2165–2170.
19. Kuyumcu-Martinez, N.M., Wang, G.S. and Cooper, T.A. (2007) Increased steady-state levels of CUGBP1 in myotonic dystrophy 1 are due to PKC-mediated hyperphosphorylation. *Mol. Cell*, **28**, 68–78.
20. Osborne, R.J., Lin, X., Welle, S., Sobczak, K., O'Rourke, J.R., Swanson, M.S. and Thornton, C.A. (2009) Transcriptional and post-transcriptional impact of toxic RNA in myotonic dystrophy. *Hum. Mol. Genet.*, **18**, 1471–1481.
21. Timchenko, L.T. (1999) Myotonic dystrophy: the role of RNA CUG triplet repeats. *Am. J. Hum. Genet.*, **64**, 360–364.
22. Timchenko, N.A., Cai, Z.J., Welm, A.L., Reddy, S., Ashizawa, T. and Timchenko, L.T. (2001) RNA CUG repeats sequester CUGBP1 and alter protein levels and activity of CUGBP1. *J. Biol. Chem.*, **276**, 7820–7826.
23. Vlasova, I.A., Tahoe, N.M., Fan, D., Larsson, O., Rattenbacher, B., Sternjohn, J.R., Vasdewani, J., Karypis, G., Reilly, C.S., Bitterman, P.B. *et al.* (2008) Conserved GU-rich elements mediate mRNA decay by binding to CUG-binding protein 1. *Mol. Cell*, **29**, 263–270.
24. Liquori, C.L., Ricker, K., Moseley, M.L., Jacobsen, J.F., Kress, W., Naylor, S.L., Day, J.W. and Ranum, L.P. (2001) Myotonic dystrophy type 2 caused by a CCTG expansion in intron 1 of ZNF9. *Science*, **293**, 864–867.
25. Cho, D.H. and Tapscott, S.J. (2007) Myotonic dystrophy: emerging mechanisms for DM1 and DM2. *Biochim. Biophys. Acta*, **1772**, 195–204.
26. Chen, W., Wang, Y., Abe, Y., Cheney, L., Udd, B. and Li, Y.P. (2007) Haploinsuffciency for Znf9 in Znf9+/− mice is associated with multiorgan abnormalities resembling myotonic dystrophy. *J. Mol. Biol.*, **368**, 8–17.
27. Raheem, O., Olufemi, S.E., Bachinski, L.L., Vihola, A., Sirito, M., Holmlund-Hampf, J., Haapasalo, H., Li, Y.P., Udd, B. and Krahe, R. (2010) Mutant (CCTG)n expansion causes abnormal expression of zinc finger protein 9 (ZNF9) in myotonic dystrophy type 2. *Am. J. Pathol.*, **177**, 3025–3036.
28. Amack, J.D. and Mahadevan, M.S. (2004) Myogenic defects in myotonic dystrophy. *Dev. Biol.*, **265**, 294–301.
29. Lafreniere, J.F., Mills, P., Bouchentouf, M. and Tremblay, J.P. (2006) Interleukin-4 improves the migration of human myogenic precursor cells in vitro and in vivo. *Exp. Cell Res.*, **312**, 1127–1141.
30. Wills-Karp, M. and Finkelman, F.D. (2008) Untangling the complex web of IL-4- and IL-13-mediated signaling pathways. *Sci. Signal.*, **1**, pe55.
31. Goetsch, S.C., Hawke, T.J., Gallardo, T.D., Richardson, J.A. and Garry, D.J. (2003) Transcriptional profiling and regulation of the extracellular matrix during muscle regeneration. *Physiol. Genomics*, **14**, 261–271.
32. Thornell, L.E., Lindstom, M., Renault, V., Klein, A., Mouly, V., Ansved, T., Butler-Browne, G. and Furling, D. (2009) Satellite cell dysfunction contributes to the progressive muscle atrophy in myotonic dystrophy type 1. *Neuropathol. Appl. Neurobiol.*, **35**, 603–613.
33. Gomes-Pereira, M., Foiry, L., Nicole, A., Huguet, A., Junien, C., Munnich, A. and Gourdon, G. (2007) CTG trinucleotide repeat 'big jumps': large expansions, small mice. *PLoS Genet.*, **3**, e52.
34. Mastroyiannopoulos, N.P., Chrysanthou, E., Kyriakides, T.C., Uney, J.B., Mahadevan, M.S. and Phylactou, L.A. (2008) The effect of myotonic dystrophy transcript levels and location on muscle differentiation. *Biochem. Biophys. Res. Commun.*, **377**, 526–531.
35. Mankodi, A., Logigian, E., Callahan, L., McClain, C., White, R., Henderson, D., Krym, M. and Thornton, C.A. (2000) Myotonic dystrophy in transgenic mice expressing an expanded CUG repeat. *Science*, **289**, 1769–1773.
36. Lefort, N., Feyeux, M., Bas, C., Feraud, O., Bennaceur-Griscelli, A., Tachdjian, G., Peschanski, M. and Perrier, A.L. (2008) Human embryonic stem cells reveal recurrent genomic instability at 20q11.21. *Nat. Biotechnol.*, **26**, 1364–1366.
37. Perrier, A.L., Tabar, V., Barberi, T., Rubio, M.E., Bruses, J., Topf, N., Harrison, N.L. and Studer, L. (2004) Derivation of midbrain dopamine neurons from human embryonic stem cells. *Proc. Natl Acad. Sci. USA*, **101**, 12543–12548.
38. Nelson, J.D., Denisenko, O. and Bomsztyk, K. (2006) Protocol for the fast chromatin immunoprecipitation (ChIP) method. *Nat. Protoc.*, **1**, 179–185.
39. Dahl, J.A. and Collas, P. (2008) A rapid micro chromatin immunoprecipitation assay (microChIP). *Nat. Protoc.*, **3**, 1032–1045.
40. Martinat, C., Bacci, J.J., Leete, T., Kim, J., Vanti, W.B., Newman, A.H., Cha, J.H., Gether, U., Wang, H. and Abeliovich, A. (2006) Cooperative transcription activation by Nurr1 and Pitx3 induces embryonic stem cell maturation to the midbrain dopamine neuron phenotype. *Proc. Natl Acad. Sci. USA*, **103**, 2874–2879.
41. Sauliere, J., Sureau, A., Expert-Bezancon, A. and Marie, J. (2006) The polypyrimidine tract binding protein (PTB) represses splicing of exon 6B from the beta-tropomyosin pre-mRNA by directly interfering with the binding of the U2AF65 subunit. *Mol. Cell Biol.*, **26**, 8755–8769.
42. Staropoli, J.F., McDermott, C., Martinat, C., Schulman, B., Demireva, E. and Abeliovich, A. (2003) Parkin is a component of an SCF-like ubiquitin ligase complex and protects postmitotic neurons from kainate excitotoxicity. *Neuron*, **37**, 735–749.